

An Inexpensive Autosampler to Maximize Throughput for an Ion Source that Samples Surfaces in Open Air

Andrew H. Grange

U.S. EPA, ORD, NERL, ESD, NHSRC, PO Box 93478, Las Vegas, NV 89193-3478

e-mail address: grange.andrew@epa.gov

phone: (702) 798-2137

fax: (702) 798-2142

Short Title: Inexpensive Autosampler for a DART/oa-TOFMS

Keywords: homeland security, autosampler, DART, throughput, time-of-flight mass spectrometer

Abstract

Rapid analysis of hundreds of wipe samples after a chemical dispersion event is essential for quickly characterizing the hazard posed to the public. An autosampler was built to pull 76 cotton swabs mounted along a 91-cm (3-foot) long, square aluminum rod in open air, through the ionizing beam of a Direct Analysis in Real Time (DART^{®1}) ion source interfaced to a time-of-flight mass spectrometer. The rod and swabs mounted on N-scale model railroad flat cars were pulled through the ion source in 7.5 min by a 7-rpm motor. Percent relative standard deviations (%RSDs) of 18.5% to 21.3% were obtained for the chromatographic peak areas of the protonated molecule. Maximum-to-minimum ratios of the areas were between 2.22 and 2.71. Measured exact masses of analyte ions were always accurate to within 1 mDa.

¹DART is a registered trademark of JEOL, USA, Inc.

Introduction

Accidental, deliberate, or weather-related dispersive events disseminate chemicals over large areas. Essential to quickly assessing the hazard posed by the chemicals is rapidly identifying the chemicals, mapping their location, and estimating the amount of chemicals at each point. After remediation, thorough documentation is required to demonstrate a successful clean-up. Hundreds of wipe samples, taken with cotton swabs, could provide the necessary data when analyzed using recently commercialized open-air ion sources interfaced to a mass spectrometer that provides exact masses of ions. To provide rapid analysis of hundreds of samples, an autosampler is required.

Autosamplers for High Performance Liquid Chromatography (HPLC)/mass spectrometry (MS) and gas chromatography (GC)/MS perform numerous sequenced mechanical events including syringe movements, solvent rinses, and sample fillings and injections requiring a combination of rotational movements or linear movements in the x, y, or z directions. Usually,

the data system software controls operation of the autosampler and its sequence of events is specified in an autosampler menu. Consequently, such autosamplers are complex, have many moving parts, incorporate electronics, and cost thousands of dollars. An autosampler for commercially available, surface sampling ion sources that bombard a surface in open air with energetic neutral molecules (Cody, et al. 2005a, 2005b, Fernandez, et al. 2006, Jones, et al. 2006, Laramée, and Cody, 2007, AccuTOF) or a sprayed solution containing ions to create analyte ions (Chen, et al. 2005, Cotte-Rodríguez, et al. 2005, Fernandez, et al. 2006, Kauppila, et al. 2006, Rodriguez-Cruz, 2006, Takáts, et al. 2004, 2005, Williams and Scrivens, 2005, Direct) that then enter a mass spectrometer for mass analysis can be much simpler as long as the ionization region is readily accessible. Only a single movement is required: transport of multiple sample surfaces through the ionizing beam. This can be achieved simply using two rails upon which a support for multiple samples is moved so that the beam impacts the sample surfaces sequentially.

Ideally, the autosampler should be inexpensive and easily constructed from off-the-shelf components using commonly available tools. Different types of sample surfaces should be accepted by the autosampler and it should be able to run large batches of samples with short time intervals between samples to fully realize the throughput made possible by sampling times of seconds. Meeting these criteria would provide a versatile, low-cost autosampler. One commercial autosampler is available, the AutoDART-96[®] (IonSense, Peabody, MA), but it relies on robotics to change samples, which requires about 30 s, and utilizes modified melting point tubes for sampling. It is not designed for rapid throughput of cotton swab wipe samples, which was the goal of our design. This paper describes and characterizes an inexpensive, easily fabricated, variable-speed autosampler for a Direct Analysis in Real Time (DART) ion source (Ion Sense, Peabody, MA) interfaced to a JEOL AccuTOF[®], orthogonal acceleration, time-of-flight mass spectrometer (oa-TOFMS) (JEOL, Peabody, MA).

Design, Dimensions, and Fabrication

The distance between the He beam source and the ion intake orifice of the mass spectrometer is adjustable up to 1.6 cm (5/8") and was set to 1.1 cm (7/16") for these experiments. This dimension provided ready passage through the beam of cotton swab heads (Puritan Medical Products, Guilford, Maine) with diameters of 0.6 - 0.7 cm (1/4 - 9/32") and of melting point tubes between 0.15 and 0.18 cm (~1/16") in diameter (VWR, West Chester, PA). Sufficient space was available between the He beam source and the oa-TOFMS to permit building of a simple autosampler based on N-scale model railroad components. Figure 1 is a photo of the DART ion source displaying the He beam source, cone orifice of the oa-TOFMS, N-scale model railroad track and flat car, a 0.64 cm (1/4")-square aluminum (Al) rod supporting cotton swabs, and two acrylic glass alignment devices. The height between the center of the beam axis and the top of the track rails was 2.9 cm (1 1/8"), and the maximum width between the base of the DART ion source and the oa-TOFMS was 2.2 cm (7/8"). These dimensions constrained the dimensions of the autosampler design.

Rails and Flat Cars.

The N-scale track (Bachmann Industries, Philadelphia, PA) provided rails with their centers 1.0 cm (25/64") apart on 1.6 cm (5/8") wide plastic ties, which were narrower than the 2.2 cm (7/8") available between by the DART and oa-TOFMS. To minimize the height required by track within the source region, 76 cm (30") segments of bare track (rather than track mounted on plastic, simulated-gravel roadbed) were used to provide 282 cm (111") of track extending 113 cm (44.5") to the left and 152 cm (60") to the right of the ion source housing as shown in Figure 2. Two 23-cm (9") re-railers mounted on plastic, simulated-gravel roadbed were included in the 152 cm track length, about 60 cm (2 feet) apart, which were used to quickly align the flat car wheels on the track. One re-railer is shown in Figure 3a. The track was tacked to a wooden support by drilling holes into the wood and press fitting the tacks through holes in the plastic ties into the drilled holes. Pre-drilled holes avoided using a hammer to install the tacks and the jolts the instrument would suffer with each hammer blow.

The flat cars (52 feet, center depressed no load, Bachmann Industries), provided the lowest height (1.0 cm [13/32"] above the rail) among the different rail car designs, leaving more vertical length available for the samples and their support. Plastic was sanded off each side of the 1.9 cm (3/4")-wide flat cars to narrow the cars to 1.75 cm (11/16"), thereby lessening the chance

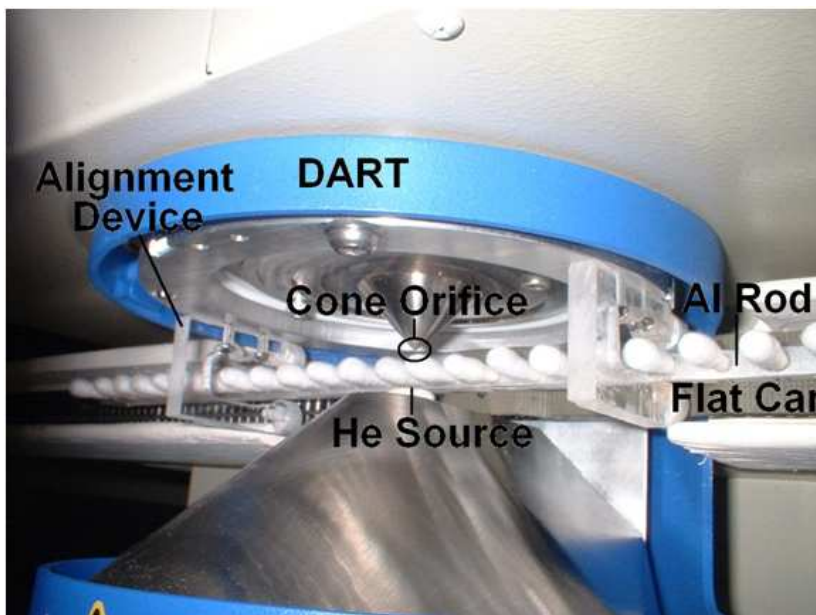


Figure 1. Top view photo of cotton swabs supported by an Al rod mounted on N-scale railroad flat cars riding on N-scale track. The rod is aligned midway between the He source and the cone orifice by guides made from acrylic glass and Al posts.



Figure 2. Photo of the track support with two slots to permit use of two re-railers that facilitate rapid mounting of the flat cars on the track.

of the cars rubbing against the DART housing when the cars passed under the ionizing beam. To minimize sag of the Al rods that support the cotton swabs, the two 10 cm (4")-long flat cars were placed as in Figure 3b such that about 30 cm (12") of the center of the rod was between the cars and the two rod ends extended 20 cm (8") beyond the cars. The slots seen in Figure 3a, 0.64 cm (1/4") wide, 2.1 cm (13/16") long, and 0.16 cm (1/16") deep, were milled on the upper flat car surfaces to prevent protruding stubs of the cotton swabs from lifting the rod and rotating it about the track axis.

Track Support.

The two horizontal sections of the track support structure shown in Figure 2 were made from pine, 113 cm (44.5-inch) and 152 cm (60 inch)-long 2 x 4's (3.8 cm x 8.9 cm [1.5" x 3.5"]). A 2.2 - 2.4 cm (7/8" - 15/16")-wide channel, 2.5 - 2.9 cm (1 - 1.25 inches) deep, was cut along the length of the 2 x 4's using a dado and 4.1 cm (1 5/8") was cut from the bottom of the channel to minimize the weight of the support. The channels prevented the user from knocking the samples and flat cars off the track and onto the floor, whereupon samples could exit the Al rod and become contaminated and mixed up. The 152 cm length provided ample distance for a 91-cm (3-foot) Al rod sample holder and a pulley, and traversed the table supporting the PC's, their displays, and the printer in Figure 2 to a vertical support. The 113 cm track-length provided room for a 91 cm rod, drive motor, and a pulley. The dado was also used to cut two additional 0.5 cm (3/8") slots in the side of the channel for the two re-railers with their plastic bases. Two 6-32 holes were tapped through each of the two side panels of the oa-TOFMS cabinet for screws that secured the track support against the cabinet to ensure it did not pull away from the instrument. This design minimized the materials needed for construction of the support.

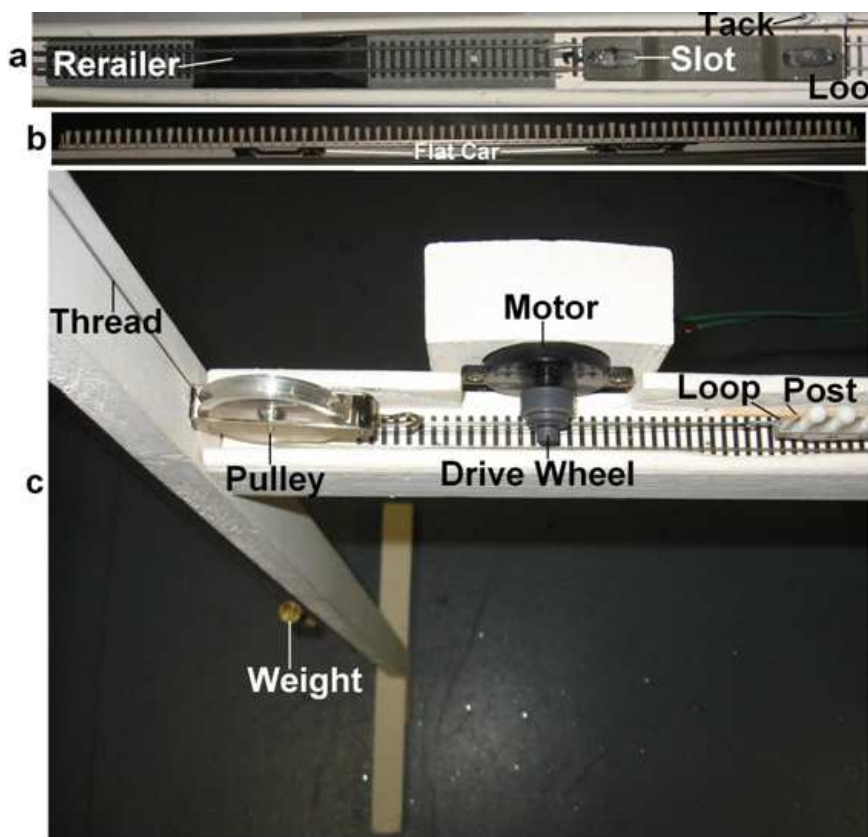


Figure 3. (a) photo of a re-railer, a flat car with milled grooves, a double loop, and a tack for parking the double loop when no Al rod is present, (b) a photo of a 91 cm Al rod with flat cars positioned to minimize rod sag, and (c) a photo of a weight, thread, a pulley, the 7-rpm motor, the drive wheel, a double loop and a post onto which one loop attaches to the Al rod.

Sample Support and Samples. As illustrated in Figure 4, 91-cm-long, 0.64 cm-square Al rods (Small Parts, Inc., Miami Lakes, FL) can be used to provide a variety of sample supports. Long sample trains maximize the throughput advantage of rapid analysis of individual samples. The configuration of the holes drilled into or through the Al rods to support individual samples and the spacing between the holes depends on the types of samples and the experiments.

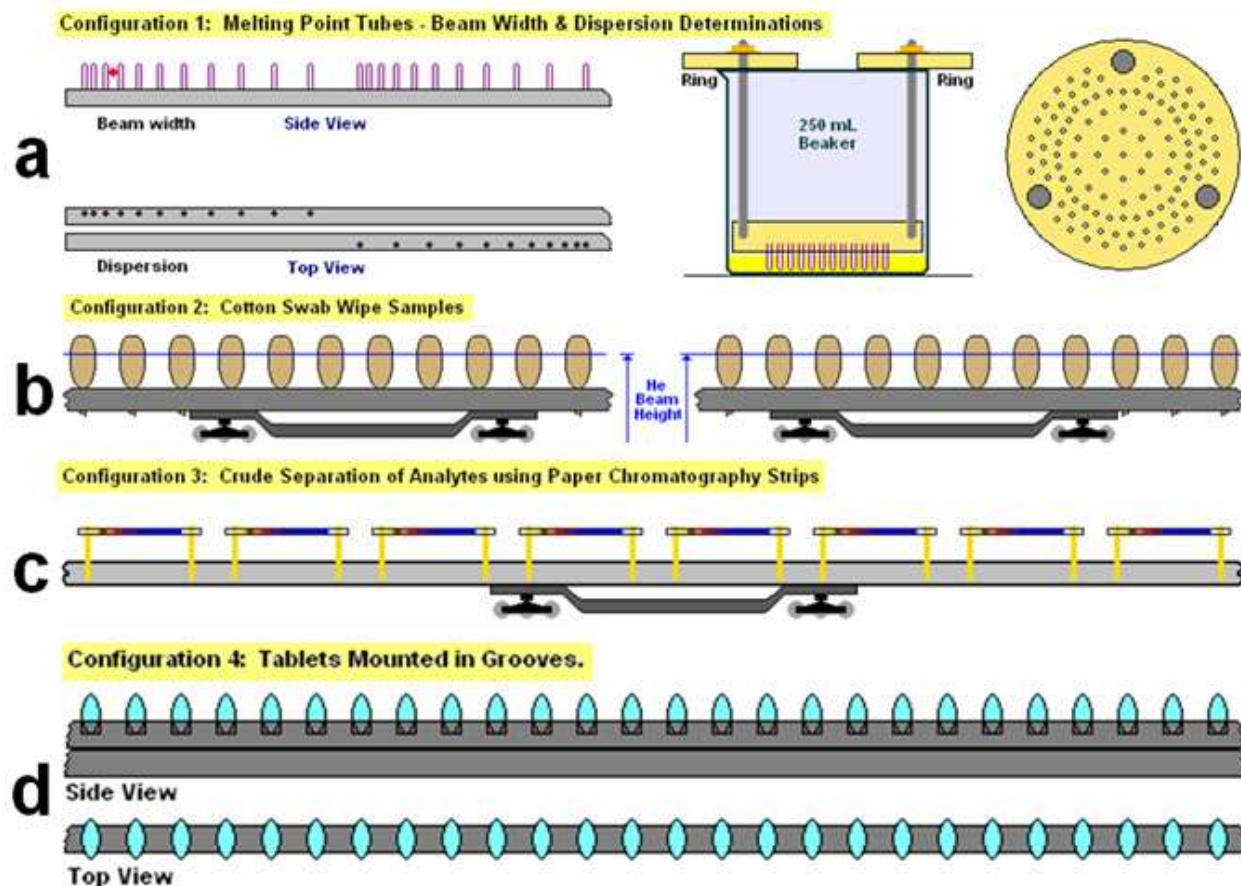


Figure 4. Al rods with (a) 0.17 cm holes 0.48 cm deep that support truncated melting point tubes and a system for dipping the tubes to ensure that the same amount of an analyte is coated onto each tube, (b) cotton swabs mounted 1.19 cm apart through 0.28 cm holes, (c) paper chromatography strips mounted horizontally on cotton swab sticks, and (d) tablets mounted in slots in the upper rod.

In Figure 4a, to support shortened melting point tubes (MPTs) with lengths of 2.2 - 2.4 cm (7/8"-15/16"), 0.17 cm (0.067") holes were drilled using a #51 drill bit 0.48 cm (3/16") deep into the Al rod at different spacings as described later. In Figure 4b, holes 0.28 cm (7/64") in diameter were drilled through the rods 1.19 cm (15/32") apart when the samples were cotton swabs. The spacing between the swabs provided for use of 1.8 mL, wide-mouth, clear-glass vials (VWR, West Chester, PA) to cover and protect each swab in a portable wipe sample transport before and after it would be used to obtain a wipe sample (Grange, 2007). In Figure 4c, analytes could be desorbed and ionized from horizontally mounted strips of chromatography paper and in Figure 4d, pharmaceutical tablets could be sampled by mounting them in slots milled into the rod. Chen, et al. designed an autosampler using a moving belt for a DESI source that analyzed

up to 16 tablets at a time (Chen, et al. 2005). The two proposed configurations depicted in Figures 4c and 4d were not investigated.

Alignment. To prevent large diameter samples such as a cotton swabs from touching the He source or the cone orifice, the alignment of the swabs along the He beam axis was controlled. Figure 5 shows a simple alignment device made from 0.64 cm (1/4")-thick acrylic glass, 1.3-cm (0.5")-diameter Al rod, and 6-32 steel machine screws. As seen in Figure 1, two of these alignment devices were affixed to the face of the oa-TOFMS by screwing them into two pairs of threaded holes already present. The two Al posts at the bottom of each device limited travel of the Al rod across the He beam axis and rotation of the rod along its longitudinal axis. The holes in the posts through which the tightening screw passed and in which the screw heads were located provided about 0.13 cm (0.050") of adjustment between the posts. To provide for easy passage of the Al rod between the posts, the first post was tightened, a labeled Al rod and two pieces of copier paper were placed between the posts, and the second post was tightened against the rod. After removing the pieces of paper the labeled Al rod passed between the stationary posts with little resistance and little tolerance for mis-location of the rod.

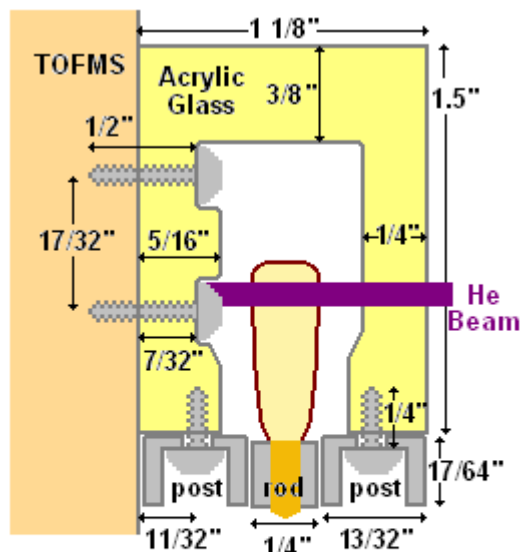


Figure 5. Cross section of an alignment device made from 0.64 cm-thick acrylic glass, 1.3-cm-diameter Al rod, and 6-32 machine screws.

To test the alignment of the Al rod before acquiring data, it was moved through both alignment devices and then backed off so that the first cotton swab or MPT was positioned about 1 cm to the right of the He beam as viewed from the front of the instrument. This was done with neither He nor N₂ flowing to minimize desorption of analytes by the gas beam or with paper blocking the gas beam before it reached the swabs. This pre-positioning ensured that the Al rod was aligned well even before the end of the Al rod reached the second pair of posts during data acquisition. As long as the ends of the sample support rod and the sides of the flat cars did not touch the sides of the channels on either side of the source, alignments of all other components of the autosampler were acceptable. A wood spacer between the base of the He beam source and the track ties ensured the sides of the flat cars did not touch the base.

Propulsion. Two means of pulling the two flat cars supporting the 91-cm Al rod were explored: an N-scale locomotive and a 7-rpm variable speed, DC motor. Unfortunately, the locomotive did not run steadily at lower speeds and required a clean track to retain electrical contact and run steadily at higher speeds.

The motor (Edmund Scientific, Tonawanda, NY) also powered by the engine's transformer, a ±15 V DC power supply (Railpower 1370, Bachmann Industries, Philadelphia,

PA), provided a wide range of constant and useful speeds. Grooves providing diameters of 0.69 cm (0.273"), 1.52 cm (0.597"), and 1.88 cm (0.742") were cut into the 1.90 cm (3/4") length of 2-cm diameter plastic rod shown in Figure 3c with a lathe and press fit onto the motor's drive shaft to provide three speed ranges. The motor provided speeds between 0.138 cm/sec at 50% power (%RSD = 0.6%, N = 3, 50.0 cm of travel) with the smallest diameter groove and 1.00 cm/sec at 100% power (%RSD = 0.4%, N = 3, 50.0 cm of travel) with the largest diameter groove.

The motor pulled the thread visible in Figure 3c. The thread was connected atop the Al rod at each end by loops fashioned from a paper clip that fit over a piece of swab stick press fit into 0.23-cm (0.089" [#43 drill bit])-diameter holes 0.3 cm (1/8") from the ends of the rod. To provide several feet of travel for the Al rod, each thread underwent two directional changes through 5-cm (1 15/16")-diameter pulleys (Palmer pulleys, Science Kit & Boreal Laboratories, Tonawanda, NY). The threads connected to weights, which were 7.0-cm (2 3/4") hex-head bolts weighing 71 g. The pulleys and 183-cm (6-foot) towers in Figure 2 made from pine 1 x 2's (1.9 cm x 3.8 cm) [0.75" x 1.5"] provided ample distance for the weights to travel as the entire Al rod passed through the ion source. The four pulleys provided minimal resistance for movement of the two weights. The weights kept the thread taut and tight against the plastic drive wheel to avoid thread slippage around the wheel. The thread was wrapped only one time around the wheel. If instead of a second pair of pulleys and weights, the thread were wound around the drive wheel, an increase in speed would occur as multiple thread windings increased the apparent diameter of the wheel. Smooth motion was provided when the motor was used to pull the rod. Steadier speeds were obtained consistently when the Al rod was pulled by the motor from right to left. To return the sampling train to its initial position, manually lifting the left weight and gently pulling on the string to the right of the pulley restored the Al rod to its starting position just to the right of the orifice more rapidly than reversing the direction of travel at any speed.

Tools and Materials Cost. Construction of the autosampler required a 10" drill press, a 10" table saw, dado, mill-lathe combination, and common hand tools. Including shipping costs where appropriate, the N-scale railroad components (track, two re-railers, transformer, two flat cars, and track joints) were purchased from a local hobby store or on-line (Discount) and cost \$85. The 7-rpm motor cost \$34, the four pulleys cost \$24, the lumber cost \$10, and the 14 Al rods cost \$60. A thousand cotton swabs cost about \$26. Screws, scrap acrylic glass, and a length of Al rod were on hand. The total cost of the autosampler materials was less than \$250.

Testing of the Autosampler

The effects of three variables associated with the autosampler on ion chromatograms were investigated: separation between melting point tubes (MPT), location of MPTs on the He beam source - cone orifice axis, and the sample speed through the beam.

Instrument conditions. The following instrument parameters were set based on values recommended by the manufacturer, found by tuning the instrument for high resolution and high ion abundance, and by limited observation of the effect of limited ranges of variables on ion abundances. These parameters were not investigated intensively and were tested in the positive-ion mode only. The instrument settings were: ring lens, 5 V; orifice 1, 15 V; orifice 2, 5 V; cone

temperature, 120°C; peaks voltage, 1000 V (to observe ions down to 100 Da); bias, 28 V; pusher bias, -0.50 V; focus voltage, -120 V; focus lens, -5 V; quadrupole lens, 6 V; right/left, -15 V; top/bottom, -2 V; reflectron, 800 V; pusher voltage, 778 V; pulling voltage, -778 V; suppress voltage, 0.20 V; flight tube, -7000 V; detector, 2300 V, He temperature, 350°C; and He flow, 3.0 L/min (to provide an audible hiss).

Mass Spectra. The mass scan range was 60 - 600 Da, although only ions with m/z 100 or greater were observed with a peaks voltage of 1000 V. Ion chromatograms integrated over a mass range of ± 50 mDa for the $[M+H]^+$ ions from three analytes obtained from Aldrich (Milwaukee, WI) were plotted to characterize the autosampler: 2-aminobiphenyl ($C_{12}H_{12}N^+$, m/z 170.09643), 2-(methylthio)benzothiazole ($C_8H_8NS_2^+$, m/z 182.00927), and N-butylbenzenesulfonamide ($C_{10}H_{16}NO_2S^+$, m/z 214.08963). With 15 V applied to orifice 1, the first two analytes provided only the protonated molecules, while the third analyte sometimes provided an ammoniated molecule in addition to the more prominent protonated molecule. Carefully positioning a swab with the third analyte inside the instrument user's wide open mouth, exhaling, and immediately acquiring data increased the relative abundance of the ammoniated mass peak. This experiment suggests that the source of the ammonia was the operator.

Ionizing beam diameter. Holding a piece of paper in a 350°C He beam provided a circular burn, but no well-defined boundary for the beam diameter. Of primary interest is the ionizing beam diameter, *i.e.*, the diameter of the He beam that produces ions. The first experiment used variable separation between MPTs and two beam-axis locations to estimate the ionizing beam diameter and to check for divergence of the He beam. As illustrated in Figure 4a, an Al rod supported five sets of eleven 0.15-0.18 cm diameter MPTs that had been dipped into 100 ng/ μ L of 2-aminobiphenyl in methanol.

The MPT batch preparation fixture shown in Figure 4a can prepare up to 106 MPTs at one time. The MPTs were press fit into 0.17 cm (0.067") holes in the plywood disc. The sealed end of the 2.2 - 2.4 cm-long MPTs were submerged to a depth of about 1.6 cm (5/8") in the methanol solution for 1 min and then lifted and allowed to dry. No MPTs fell out of the disk during this process.

As illustrated in Figure 4a, the MPTs were mounted in the Al rod with increasing distances between the walls of adjacent MPTs of 0.08 cm (1/32") to 0.79 cm (5/16") at 0.08 cm (1/32") increments. Each 11-MPT set was pulled along the track at the slowest speed available. A single data acquisition was made while all 55 MPTs passed through the He beam as the 91-cm Al rod was pulled through the DART ion source. The Al rod was run twice with freshly coated MPTs closer to the cone orifice or to the He source to check for He-beam dispersion. The distance between the He source and cone orifice was 1.1 cm (7/16"). The centers of the MPTs supported by the Al rod were located 0.36 cm (9/64") from the cone orifice for the ion chromatogram in Figure 6a and the same distance from the He source for Figure 6b.

The baseline was observed when the ionizing beam traversed only air or when an object blocked its path. Because only one chromatographic peak was observed for well-separated

MPTs, the width of the MPTs was less than that of the ionizing beam. Otherwise, no signal would have been observed when the MPT blocked the He beam from reaching the cone orifice.

The ionizing beam diameter was estimated from Figure 6. Because the distance between adjacent MPT tubes 1, 2, and 3 was smaller than the ionizing He beam diameter, the beam sampled two MPTs at once, and analyte ions from two MPTs contributed to the chromatographic peak area. Conversely, the distance between MPTs 3, 4, ..., 11 was wider than the ionizing He beam, and the baseline was observed while the beam passed between the MPTs. To minimize the distance traveled during the data accumulation period for each scan and thereby maximize spatial resolution, 10 scans/sec and a speed of 0.138 cm/sec were used. The Al rod traveled 0.0138 cm (0.005") during each scan.

In Figure 6, the baseline was first observed between MPTs 3 and 4 during both data acquisitions for all five sets of MPTs. The sides of the MPTs were separated by 0.24 cm (3/32"). As illustrated in Figure 7, the MPTs traveled 0.0138 cm during the first scan and the same distance during the second scan. In addition, the distance of a third scan is taken into account since the start of the first scan need not coincide with the beam just missing the side of the left MPT. Thus, the intra-MPT distance was up to 0.04 cm wider than the ionizing He beam diameter. This distance subtracted from 0.24 cm yields 0.20 cm as the ionizing beam width near the cone. The estimated maximum error in the measured distance between the two MPTs was ± 0.04 cm (1/64"). Hence, the ionizing beam width was estimated to be 0.20 ± 0.04 cm. For distances between surfaces of at least 0.24 cm, analyte ions will be collected from only one sample at a time when the sample speed is 0.138 cm/s.

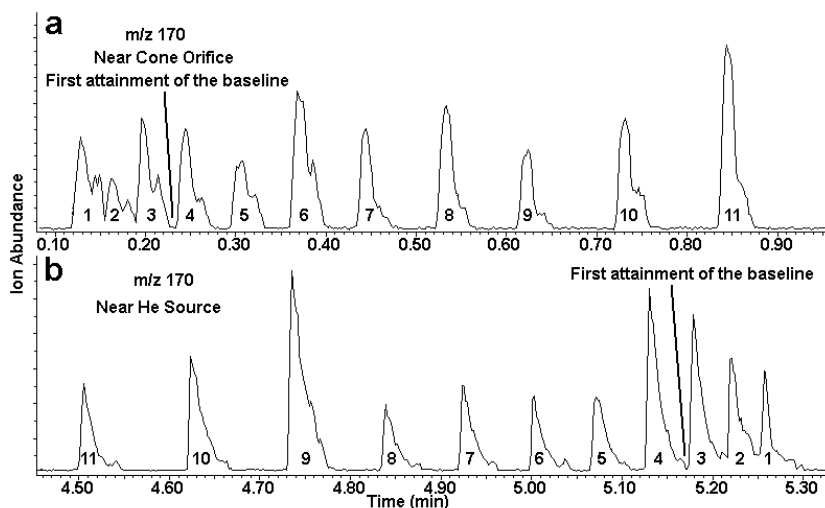


Figure 6. Ion chromatogram for the $[M+H]^+$ ion from 2-aminobiphenyl (a) for the Al rod configuration with the MPTs closer to the cone orifice and (b) for the configuration with the MPTs closer to the He source.

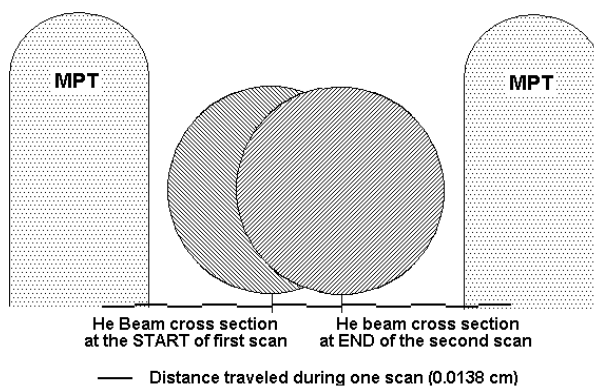


Figure 7. Graphical representation of two MPTs and the relative position of the fixed He beam passing between them after two scans. Each horizontal line segment represents the distance traveled by the Al rod during a scan (0.0138 cm).

Because the baseline was observed between MPTs 3 and 4 for both He beam axis locations, beam divergence was not detected by this experiment over a distance of 0.40 cm (5/32") along the He beam axis. The average ion abundance was 22% greater and the shoulders

on the chromatogram peaks were less pronounced for the MPT placement nearer the He source. A thermocouple and multi-meter (Extech Instruments, Radio Shack, Fort Worth, TX) measured 334°C in the center of the He beam at the He source and 298°C at the orifice. Apparently, the hotter beam more completely and rapidly desorbed analyte from the MPT. In addition, the He beam near its source contains more metastable He and/or reagent ions than near the cone orifice, which could produce more analyte ions from MPTs closer to the He source.

Scan and Sample Speeds. Holes in the center of the Al rod shown in Figure 4b positioned cotton swab heads midway between the He beam source and the cone orifice, thereby minimizing the chance of an off-center swab head touching either. Before swabs were inserted through the holes, they were dipped into methanol for about 6 s and immediately rolled across a table top for a distance of about 50 cm to simulate collection of a wipe sample. The fastest scan speed recommended by the manufacturer, 10 scans/sec, was used to provide the best available chromatographic resolution. Several sample speeds were investigated. As the sample speed was decreased, the relative standard deviation (RSD) decreased for the 72 analyte swabs and the chromatographic peak areas increased. Chen *et al.* also noted a reduction in RSDs at slower speeds using a moving belt to carry 16 pharmaceutical tablets through a DESI source (Chen, *et al.* 2005).

Figure 8a displays an ion chromatogram acquired with the rod moving at 0.20 cm/sec for the base peak from 2-aminobiphenyl for 72 swabs, and Figure 8b shows a portion of the ion chromatogram magnified along the x-axis. In Figure 8b, all six chromatographic peaks (two for each swab) are delineated by at least four scans and a well defined baseline is reached between the swab signals. These observations were not true for higher sample speeds. The %RSDs for the summed pairs of chromatographic peak areas

from each swab for five 72-swab sets, two sets for m/z 170, one set for m/z 182, and two sets for m/z 214 were 18.5%, 21.3%, 20.0%, 20.9%, and 20.0%, respectively. The corresponding maximum/minimum area ratios were 2.22, 2.28, 2.41, 2.45, and 2.71. These measures of precision include the effects of variable swab head size and shape, variation in the seating within the holes in the Al rod, formation of cotton tufts caused by the 3 L/min He beam, and instrument variations. The data acquisition for 72 analyte swabs and four calibrant swabs required about 7.5

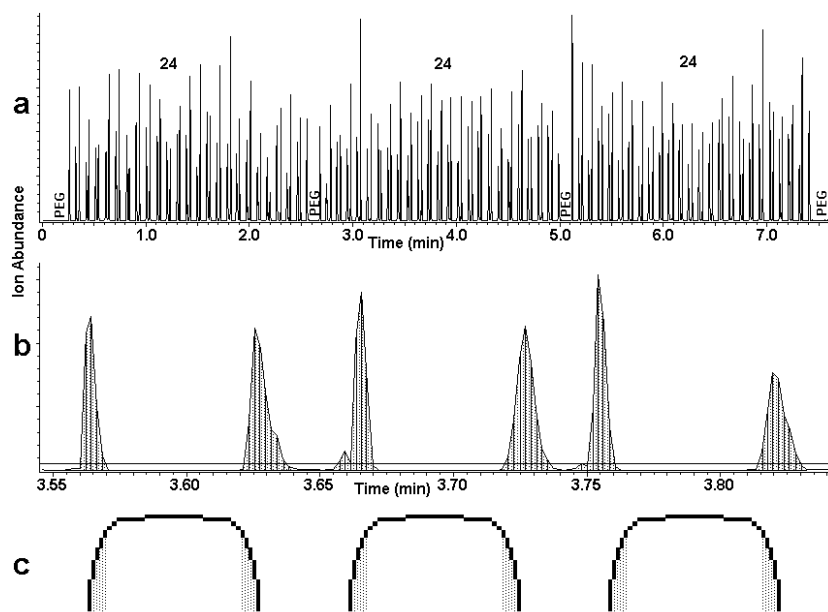


Figure 8. Ion chromatograms for the $[M+H]^+$ ion from 2-aminobiphenyl (a) for 76 cotton swabs, four of which are calibrant swabs that provide no m/z 170 ion abundance (b) for a magnified portion of the ion chromatogram for three swabs, and (c) a graphical representation of the positions of the swabs relative to the signals observed. The horizontal line above the x-axis in (b) corresponds to 20 times the average baseline.

min. For our proposed application of preparing semi-quantitative dispersion maps of chemicals based on up to 1000 wipe sample analyses during one day, 0.20 cm/sec provided the best combination of reproducibility, sensitivity, and speed.

Chromatographic Peak Shape. In Figure 8b, each swab provides two chromatographic peaks: one as the He beam grazes first the leading edge (left side) of the swab and a second as the beam grazes the trailing edge (right side). Between these peaks, the bulk of the swab and the support stick blocked ions from reaching the cone orifice, and the signal was cut off to provide a sharp right side for the peaks from the leading edge of the swabs and from the left side of the peaks from the trailing edge of the swabs. The beam traversed open space between the swabs. The chromatographic peaks from the trailing edge of swabs were wider. It is possible that the temperature necessary to desorb analytes is not reached immediately as the He beam strikes the leading edge of each swab, while for the trailing edge, the hot He beam has preheated the cotton such that analyte desorption occurs for a longer period. This would explain the wider chromatographic peaks for the trailing edge of the swabs.

Data Processing. To determine chromatographic peak areas for each swab, an ion chromatogram was saved by the oa-TOFMS data system as an ASCII file of data acquisition times and corresponding ion abundances (*.JMC file). The *.JMC file was imported into a LOTUS[®] 123 version 9.6 spreadsheet (IBM, Armonk, NY) as numbers. A baseline estimate was determined as the average for the first 10 scans and the beginning and end of each chromatographic peak was usually taken as 20 times this value. The horizontal line above the x-axis in Figure 8b corresponds to 20 times the average baseline. For increasing scan numbers, once this threshold was exceeded, the ion abundances were summed until the ion abundance for a scan fell below this level to provide the area of each chromatographic peak. Rare small peaks observed between the two peaks for each swab were ignored if their area was less than 15% of the maximum ion abundance observed for all 144 chromatographic peaks. This simple algorithm usually ensured areas were found for 144 peaks in each data file obtained using a sample speed of 0.20 cm/s. When fewer or more than 144 peaks were found, manual interpretation became necessary to correctly correlate chromatographic peaks with their swabs. The program also summed the areas of the two chromatographic peaks observed for each of the 72 analyte swabs.

Repetitive Data Acquisitions. Each side of a swab provides signal for 0.5 - 1.5 s. One set of 72 analyte swabs dipped into 100 ng/ μ L of 2-aminobiphenyl in methanol and run four times yielded average paired chromatographic peak areas for the m/z 170 ion in the ratio 1.00, 0.69, 0.57, and 0.48. A second set of 72 analyte swabs dipped into 100 ng/ μ L of 2-(methylthio)benzothiazole in methanol and run four times yielded average paired chromatographic peak areas for the m/z 182 ion in the ratio 1.00, 0.75, 0.60, and 0.54. Sufficient analyte remains after each run to permit other ionization conditions to be investigated. For example, the negative ionization mode could be tried, a swab dipped into an ammonium hydroxide solution could be placed near the He beam to check for formation by analytes of ammonium adduct ions in the positive mode, or a swab near the beam dipped into methylene chloride could provide chloride adduct ions in the negative mode. The ionization conditions providing the largest signal for a given analyte should be used.

Specificity. Accurate exact masses are critical when compounds must be identified. Initial use of a calibration solution containing PEG 600 and four compounds to provide lower-mass calibration ions, chlorpromazine (an oxidized ion, $[M+OH]^+$, $C_{17}H_{20}ClN_2OS^+$, m/z 335.09794), carbamazepine ($[M+H]^+$, $C_{15}H_{13}N_2O^+$, m/z 237.10224), caffeine ($[M+H]^+$, $C_8H_{11}N_4O_2^+$, m/z 195.08765), and pseudoephedrine ($[M+H]^+$, $C_{10}H_{16}NO^+$, m/z 166.12264) ensured exact masses accurate to within ± 1 mDa were measured. A 99:1 methanol: PEG 200 solution was also found to provide excellent calibration for the low-mass (170 - 214 Da) ions studied. A mass accuracy of ± 1 mDa provides excellent specificity and minimizes the possibility of falsely identifying other compounds that provide the same nominal mass as the analyte. When multiple compositions are still possible for an ion within a 1 mDa error limit, the relative isotopic abundances of the ions heavier by 1 and 2 Da than the monoisotopic ion provide an independent physical property of elements for distinguishing among them (Grange, et al. 2006).

Calibration Drift. Calibration drift might depend on several variables including the warm up time for the instrument, the temperature variation in the laboratory, and line voltage variation, all of which might differ for each data acquisition. The importance of the last two factors is laboratory specific. Figure 9a shows the mass errors for the m/z 182 ion from 100

ng/ μ L of 2-(methylthio)benzothiazole in methanol referenced against calibrant ions from the calibrant swab in the first position on the Al rod, and Figure 9b shows the mass errors when the analyte swab spectra were calibrated against the calibrant swab closest in time. The calibrant swabs in positions 1, 26, 51, and 76 were used to calibrate the analyte swabs in positions 2-13 (12 swabs), 14-25 and 27-38 (24 swabs), 39-50 and 52-63 (24 swabs), and 64-75 (12 swabs), respectively .

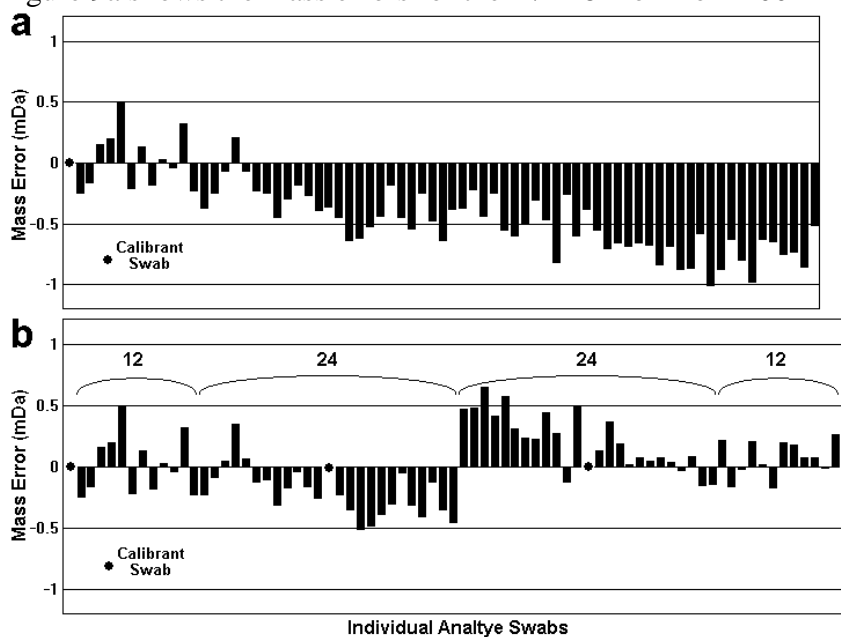


Figure 9. Mass errors when the m/z 182 ion from 72 analyte swabs was calibrated against (a) the first calibrant swab and (b) the calibrant swab closest in time

From the average mass errors for the first 12 and last 12 analyte swabs, a calibration drift of -0.95 mDa occurred over the 7.5 min data acquisition. This negative calibration drift is evident in Figure 9a. The largest error was -1.01 mDa. When the maximum drift time between acquisition of the calibrant and analyte mass spectra was limited to no more than 1.3 min, mass errors were smaller (-0.51 to + 0.65 mDa) as seen in Figure 9b. Using this autosampler with a

sample speed of 0.20 cm/s and four calibration swabs, the mass error is usually less than 0.5 mDa and always less than ± 1 mDa.

Conclusions

A simple autosampler providing variable-speed, linear motion of samples through an open-air ion source was constructed from less than \$250 worth of N-scale model railroad parts, a 7-rpm motor, aluminum rods, four pulleys, lumber, acrylic glass, and screws. The autosampler pulled 76 cotton swabs mounted on a 3-foot, 1/4"-square aluminum rod in open air through the He ionizing beam of a Direct Analysis in Real Time (DART) ion source for an orthogonal acceleration, time-of-flight mass spectrometer. Two alignment devices limited movement of the Al rod along the He beam axis and rotation of the rod about its longitudinal axis. Mass spectra were provided from analytes on 72 swabs and a calibrant solution containing PEG on four analyte swabs in positions 1, 26, 51, and 76. An optimum speed of 0.20 cm/s provided single data acquisition times of 7.5 min for the 76 swabs.

Use of four calibrant swabs provided external mass calibration for analyte mass spectra against calibrant mass spectra obtained no more than 1.3 min earlier or later. Exact masses were always accurate to within 1 mDa, and usually to within 0.5 mDa.

Five sets of swabs were dipped for 10 s into 100ng/ μ L of 2-aminobiphenyl (m/z 170), 2-(methylthio)benzothiazole (m/z 182), or N-butylbenzenesulfonamide (m/z 214) in methanol and allowed to dry. The %RSDs for the areas of the pair of chromatographic peaks from each swab in the ion chromatogram for the protonated molecule for the five swab sets were between 18.5% and 21.3% and the ratios of the maximum to the minimum chromatographic peak areas from each swab fell between 2.22 and 2.71. These variations arose from differences in the cotton swabs, their positioning in the holes in the swab support rod, creation of cotton tufts extending beyond the original boundaries of the swab heads by the He beam, and instrumental precision. These two measures of precision suggest that semi-quantitation into low, medium, and high levels differing by factors of at least 10 might be feasible using the autosampler with cotton swab wipe samples.

Notice: The U.S. Environmental Protection Agency through its Office of Research and Development funded and managed the research described herein. It has been subjected to Agency review and approved for publication.

References

AccuTOF™ DART™ Direct Analysis in Real Time Time-of-Flight Mass Spectrometer
<http://www.jeol.com/tabid/141/Default.aspx>

Chen, H., N. N. Talaty, Z. Takats, and R. G. Cooks. 2005. Desorption Electrospray Mass Spectrometry for High-Throughput Analysis of Pharmaceutical Samples in the Ambient Environment. *Anal. Chem.* 77: 6915-6927.

Cody, R. B., J. A. Laramée, and H. D. Durst. 2005a. Versatile New Ion Source for the Analysis of Materials in Open Air under Ambient Conditions. *Anal. Chem.* 77: 2297-2302.

Cody, R. B., J. A. Laramée, J. M. Nilles, and H. D. Durst. 2005b. Direct Analysis in Real Time (DART[™]) Mass Spectrometry. *JEOL News* 40: 8-12.

Cotte-Rodríguez, I., Z. Takats, N. Talaty, H. Chen, and R. G. Cooks. 2005. Desorption Electrospray Ionization of Explosives on Surfaces: Sensitivity and Selectivity Enhancement by Reactive Desorption Electrospray Ionization. *Anal. Chem.* 77: 6755-6764.

Direct Electrospray Ionization (DESI) <http://www.prosolia.com/DESI.html>

Discount Trains Online <http://www.discounttrainsonline.com/n-scale-model-trains.html>

Fernandez, F. M., R. B. Cody, M. D. Green, C. Y. Hampton, R. McGready, S. Sengaloundeth, N. J. White, and P. N. Newton. 2006. Characterization of Solid Counterfeit Drug Samples by Desorption Electrospray Ionization and Direct-analysis-in-real-time Coupled to Time-of-flight Mass Spectrometry. *ChemMedChem* 1: 702-705.

Grange, A.H. and G.W. Sovocool. 2006. Determination of Ion and Neutral Loss Compositions and Deconvolution of Product Ion Mass Spectra Using an Orthogonal Acceleration, Time-of-Flight Mass Spectrometer and an Ion Correlation Program. *Rapid Commun. Mass Spectrom.* 20: 89-102.

Grange, A. H. 2007. An Integrated Wipe Sample Transport/Autosampler to Maximize Throughput for a DART/oa-TOFMS. *Environmental Forensics* XX: YY-ZZ.

Jones, R.W., R. B. Cody, and J. F. McClelland. 2006. Differentiating Writing Inks Using Direct Analysis in Real Time Mass Spectrometry. *J. Forensic Sci.* 51: 915-918.

Kaupila, T. J., J. M. Wiseman, R. A. Ketola, T. Kotiaho, R. C. Cooks, and R. Kostianen. 2006. Desorption Electrospray Ionization Mass Spectrometry for the Analysis of Pharmaceuticals and Metabolites. *Rapid Commun. Mass Spectrom.* 20: 387-392.

Laramée, J. A. and R. B. Cody. 2007. Chemi-Ionization and Direct Analysis in Real Time (DART[™]) Mass Spectrometry. In the *Encyclopedia of Mass Spectrometry*, Vol. 6, 377-387. Elsevier.

Rodriguez-Cruz, S. E. 2006. Rapid Analysis of Controlled Substances using Desorption Electrospray Ionization Mass Spectrometry. *Rapid Commun. Mass Spectrom.* 20:53-60.

Takáts, Z., J. M. Wiseman, and R. G. Cooks. 2005. Ambient Mass Spectrometry Using Desorption Electrospray Ionization (DESI): Instrumentation, Mechanisms and Applications in Forensics, Chemistry, and Biology. *J. Mass Spectrom.* 40: 1261-1275.

Takáts, Z., J. M. Wiseman, B. Gologan, R. G. Cooks. 2004. Mass Spectrometry Sampling Under Ambient Conditions with Desorption Electrospray Ionization. *Science* 306: 471-473.

Williams, J. P. and J. H. Scrivens. 2005. Rapid Accurate Mass Desorption Electrospray Ionisation Tandem Mass Spectrometry of Pharmaceutical Samples. *Rapid Commun. Mass Spectrom.* 19: 3643-3650.